Eur. Phys. J. C (2014) 74:2707
DOI 10.1140/epjc/s10052-013-2707-0

THE EUROPEAN PHYSICAL JOURNAL C

Regular Article - Theoretical Physics

Large Hadron Collider constraints on a light baryon-number violating sbottom coupling to a top and a light quark

B. C. Allanach, S. A. Renner[a]

DAMTP, CMS, University of Cambridge, Wilberforce Road, Cambridge CB3 0WA, UK

Received: 11 November 2013 / Accepted: 12 December 2013 / Published online: 28 January 2014

Abstract We investigate a model of R-parity violating (RPV) supersymmetry in which the right-handed sbottom is the lightest supersymmetric particle, and a baryon-number violating coupling involving a top is the only non-negligible RPV coupling. This model evades proton decay and flavour constraints. We consider in turn each of the couplings λ''_{313} and λ''_{323} as the only non-negligible RPV coupling, and we recast a recent LHC measurement (CMS top transverse momentum $p_{\mathrm{T}}(t)$ spectrum) and a LHC search (ATLAS multiple jet resonance search) in the form of constraints on the mass–coupling parameter planes. We delineate a large region in the parameter space of the mass of the sbottom ($m_{\tilde{b}_R}$) and the λ''_{313} coupling that is ruled out by the measurements, as well as a smaller region in the parameter space of $m_{\tilde{b}_R}$ and λ''_{323}. A certain region of the $m_{\tilde{b}_R}-\lambda''_{313}$ parameter space was previously found to successfully explain the anomalously large $t\bar{t}$ forward–backward asymmetry measured by Tevatron experiments. This entire region is now excluded at the 95 % confidence level (CL) by CMS measurements of the $p_{\mathrm{T}}(t)$ spectrum. We also present $p_{\mathrm{T}}(t\bar{t})$ distributions of the Tevatron $t\bar{t}$ forward–backward asymmetry for this model.

1 Introduction

Supersymmetry (SUSY) is a beyond the Standard Model (BSM) theory that answers some of the unsolved questions of the Standard Model. In particular, weak scale SUSY provides a solution to the hierarchy problem, which is the problem of explaining how the Higgs boson mass is stable under radiative corrections which would otherwise tend to bring it up to huge values in the absence of any new physics beyond the Standard Model. However, there has been no significant evidence for supersymmetry so far at the LHC. One possible reason for this might be that most of the LHC searches have been looking for R-parity conserving supersymmetry, which implies a stable lightest supersymmetric particle (LSP). This LSP would escape the detector undetected, and so searches for this variety of supersymmetry at the LHC rely on signatures with large missing transverse momentum. Stringent cuts on the missing transverse momentum are usually imposed for these analyses. However, if supersymmetry is instead R-parity violating (RPV), it can evade these searches because the LSP is not stable, so there is no large missing transverse momentum. One argument offered for R-parity conservation is that it ensures that the proton is stable, but RPV SUSY can also avoid getting into trouble with lower bounds on proton lifetimes if either baryon number or lepton number is violated, but not both (proton decay would rely on both being present). Recently, it has also been realised that, by considering flavour symmetries and adding some extra fields charged under such symmetries, a baryon-number violating model may also be consistent with stable dark matter constraints [1]. Depending on the flavour structure of the baryon-number violating couplings, the gravitino has been shown to be a viable dark matter candidate in the R-parity violating MSSM with lifetimes long enough to evade certain bounds [2]. Thus another argument for R-parity conservation (that it guarantees a dark matter candidate) is seen to be avoidable.

If only baryon-number violating operators are present, then decays of superpartners will produce jets, which might hide amongst large quantum chromodynamics (QCD) backgrounds at the LHC. The general difficulty of discovering baryon-number violating SUSY amongst QCD backgrounds is a well-known one; many papers have discussed this problem and suggested methods involving studying jet substructure for distinguishing jets produced through BSM processes [3,4]. Other suggested analyses have relied on leptons produced in sparticle cascades (for example, Ref. [5]). The tendency of baryon-number violating SUSY to 'hide' in QCD backgrounds, along with the fact that it is expected that third generation squarks should be light to make the theory more natural [6], has led to the suggestion that baryon-number

[a] e-mail: sar67@cam.ac.uk

violating SUSY with light third generation squarks should be the next new physics scenario to search for, given the lack of SUSY signals at the LHC so far [7–11].

The RPV superpotential within the minimal supersymmetric standard model (MSSM) contains the B-violating term

$$W = \frac{1}{2}\lambda''_{ijk} U^c_i D^c_j D^c_k, \tag{1}$$

where i, j, k are family indices, U^c_i and D^c_j are chiral superfields containing the charge-conjugated right-handed up and down type quarks, respectively, and we have suppressed gauge indices. The couplings λ''_{ijk} are antisymmetric in the last two indices due to the $SU(3)$ colour structure. This superpotential term can be rewritten in terms of the component fields as

$$L_{\not B} = \lambda''_{ijk}(u^c_i d^c_j \tilde{d}^*_k + u^c_i \tilde{d}^*_j d^c_k + \tilde{u}^*_i d^c_j d^c_k) + h.c., \tag{2}$$

where lower case fields are left-handed Weyl fermions unless they have a tilde, in which case they are scalars. If third generation squarks are light, couplings of third generation squarks to quarks in the proton, i.e. couplings of the form λ''_{3jk} or λ''_{jk3}, will provide new physics signals at the LHC.

Some recent works have built RPV models with minimal flavour violation [12–15] or product group unification [16] in order to provide natural models that evade LHC constraints more easily than R-parity conserving ones. General features of these models include a $U^c_i D^c_j D^c_k$ operator involving a top (s)quark as the dominant RPV operator, and a flavour mass hierarchy which predicts one of the third generation squarks as a likely LSP. The set up we investigate has these features.

In this paper we will consider the RPV couplings λ''_{313} and λ''_{323}, which are involved in the vertices shown in Fig. 1. We will consider each coupling separately, while setting the other, and all remaining RPV couplings, to zero. We will assume that the right-handed sbottom is the (unstable) LSP, and work in a simplified model in which all other superpartners are set to have very large masses. The reason for this assumption is simplicity of the parameter space: the only relevant parameters for our model are the sbottom mass $m_{\tilde{b}_R}$ and the RPV coupling λ''_{313} or λ''_{323}. Our analysis should cover a wide range of cases where various sparticles are brought down in mass, but they do not result in significant top production. One significant caveat could be the case in which gluinos and stops are lighter than 1.5 TeV, since then the production of $\tilde{g}\tilde{g}$, where each gluino decays via first SUSY QCD $\tilde{g} \to t\tilde{t}$ followed by the RPV decay of $\tilde{t}$ into two jets, would result in significant additional inclusive top production and affect our results. This, however, would depend upon the branching ratio of the gluino decay into stops: if this were small, then our analysis could still apply. A priori, it is important that the sbottom is the LSP in our scenario, otherwise competing R-parity conserving decays of the sbottom could play a role, possibly weakening our constraints. However, we shall return to this point later, arguing that, to a good approximation, our analysis should be insensitive to the identity of the LSP. The RPV couplings we consider will have large $\sim\mathcal{O}(1)$ magnitudes; therefore our analysis should still hold in the presence of other B-violating RPV couplings that are small compared to this (i.e. <0.3 or so). In general, there are flavour constraints on RPV couplings coming from measurements of flavour-changing neutral currents (FCNCs) and meson mixing [17]. These imply that other λ''_{ijk} couplings must be small, for example the particularly strict bound $\lambda''_{313}\lambda''_{323} < 0.01$ coming from $K^0 - \bar{K}^0$ mixing constraints for sparticle masses less than 1 TeV [18]. However, if we assume that there is only one non-negligible real RPV coupling, these constraints are evaded because no tree-level FCNCs are induced. Electric dipole moment constraints [17], which can become important if there are several non-negligible complex RPV couplings, are also not constraining here. In general there are strong constraints coming from atomic parity violation measurements, for example in cesium (^{133}Cs) [19]. But Dupuis and Cline have pointed out in their paper [20] that these constraints can be evaded if there is a sizeable amount of $\tilde{t}$-squark mixing, because two contributing diagrams will then cancel each other, allowing the model to pass the constraints coming from atomic parity violation. While we have set the stops to be heavy for our analysis, they could be made lighter to satisfy the atomic parity violation constraints, while not significantly affecting our predictions.

The DØ and CDF experiments at the Tevatron have measured a forward–backward asymmetry in $t\bar{t}$ events [21–24]. This is not explained by the Standard Model alone, which predicts a significantly smaller value for the asymmetry [25]. Many proposals were offered for new physics scenarios that could explain the enhanced asymmetry, see Refs. [26–29] for some examples. In 2012, Allanach and Sridhar proposed one possible explanation for this enhanced $t\bar{t}$ asymmetry using RPV supersymmetry [30]. They showed that an extra diagram contributing to $t\bar{t}$ production involving t-channel exchange of a right-handed sbottom which couples to top and down quarks via the λ''_{313} coupling (as shown in Fig. 2) could produce an asymmetry which agrees with the Tevatron

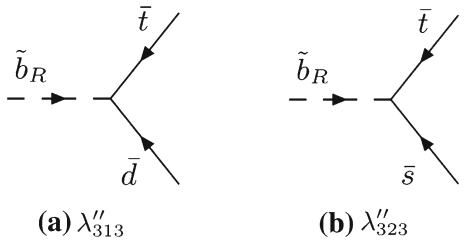

(a) λ''_{313} **(b)** λ''_{323}

Fig. 1 Relevant vertices involving the λ''_{313} and λ''_{323} couplings

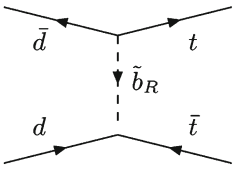

Fig. 2 Diagram of a BSM matrix element producing a $t\bar{t}$ pair (of order λ''^2_{313})

measurements. They checked their model against measurements of the $t\bar{t}$ charge asymmetry at the LHC [31] and total cross-section measurements for a range of values of the sbottom coupling λ''_{313} (to right-handed down and top quarks) and sbottom mass $m_{\tilde{b}_R}$, and found an allowed region for the model in this parameter space. Around the same time as Allanach and Sridhar's paper, Dupuis and Cline proposed the same model [20] to explain the $t\bar{t}$ asymmetry, and Hagiwara and Nakamura proposed a very similar model phrased in terms of diquarks [32]. All three papers found approximately compatible allowed regions in mass–coupling space to explain the asymmetry.

In this paper we recast recent LHC measurements in terms of constraints upon the $m_{\tilde{b}_R} - \lambda''_{313}$ parameter space and (separately) the $m_{\tilde{b}_R} - \lambda''_{323}$ parameter space. The disfavoured region in the $m_{\tilde{b}_R} - \lambda''_{313}$ parameter space includes Allanach and Sridhar's region that could explain the $t\bar{t}$ asymmetry whilst evading other collider constraints.

The paper is organised as follows: we begin in Sect. 2 by looking at the $p_{\mathrm{T}}(t\bar{t})$ dependence of the $t\bar{t}$ forward–backward asymmetry as measured by the CDF experiment at the Tevatron, and compare this to the predictions of the sbottom model. In Sect. 3 we reinterpret LHC measurements and calculate excluded regions in mass–coupling parameter spaces of the sbottom. We conclude in Sect. 4.

2 Top pair transverse momentum distribution of the forward–backward asymmetry

Last year the CDF experiment at the Tevatron measured the top quark forward–backward asymmetry as a function of kinematic properties of the event, for $t\bar{t}$ events produced by proton–antiproton collisions at a centre of mass energy of 1.96 TeV [33]. The $t\bar{t}$ forward–backward asymmetry at CDF, $A_{FB}(t\bar{t})$, is defined

$$A_{FB}(t\bar{t}) = \frac{N(\Delta y > 0) - N(\Delta y < 0)}{N(\Delta y > 0) + N(\Delta y < 0)}, \tag{3}$$

where $\Delta y = y_t - y_{\bar{t}}$, and y_t and $y_{\bar{t}}$ are the rapidities of the top and anti-top, respectively.

In particular, CDF measured the forward–backward asymmetry as a function of the transverse momentum (p_{T}) of the top anti-top pair. A non-zero p_{T} occurs when the $t\bar{t}$ system recoils against an additional jet, for example. This measurement gives new information to compare to different BSM models which attempt to explain the forward–backward

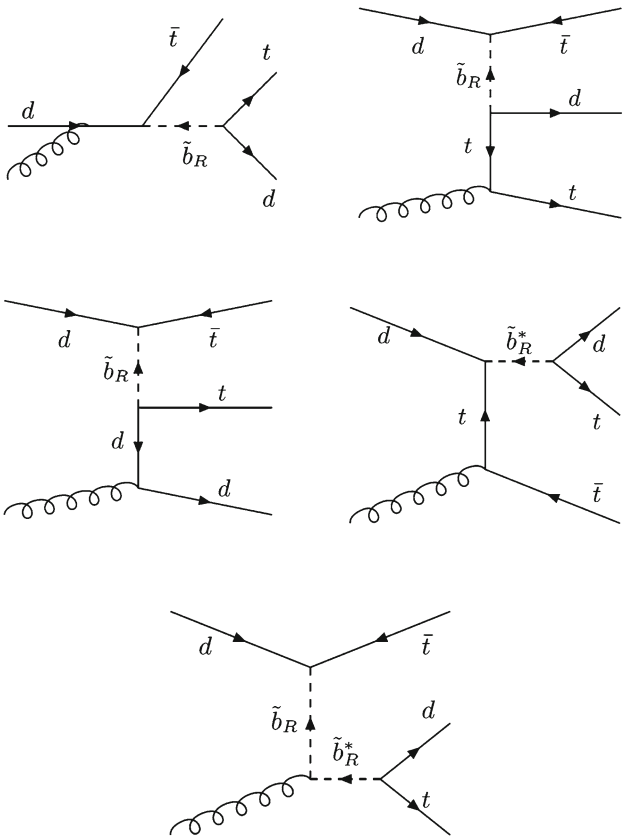

Fig. 3 Diagrams producing a $t\bar{t}$ pair as well as an extra down quark (order $\alpha_s\lambda''^2_{313}$). Not shown, but included in our simulations, are diagrams that can be created from these ones by replacing quarks with corresponding anti-quarks, and vice versa

asymmetry. In fact, both colour octet (for example axigluon exchange) models and colour singlet models (for example, Z' exchange) were recently shown to have rather flat differential distributions of $A_{FB}(t\bar{t})$ with $p_{\mathrm{T}}(t\bar{t})$ [34]. The predictions from t-channel colour anti-triplet exchange have not appeared in the literature, and so we provide them here.

Here, using `MadGraph5_v1_5_11` [35] with the FeynRules [36] implementation of the RPV MSSM [37,38], we calculate the distribution for the RPV SUSY model with λ''_{313} as the non-zero RPV coupling. We simulate all processes that produce a $t\bar{t}$ pair plus a jet; i.e. the diagram in Fig. 2 with emission of an additional gluon, and also the diagrams in Fig. 3, as well as the leading-order QCD processes for $t\bar{t}$ plus jet production (and interference between BSM and QCD diagrams). Our simulations were performed at parton level and we did not decay tops, nor did we include parton showering. We simulated 25 million events for each histogram. CDF give their results unfolded to the parton level, so that they can be directly compared to theoretical parton level predictions.

Figure 4 shows the CDF measurement along with the leading-order predictions of `MadGraph5_v1_5_11` [35] for a sbottom mass of 600 GeV and two different values of the coupling λ''_{313}, and for a sbottom mass of 1,100 GeV and

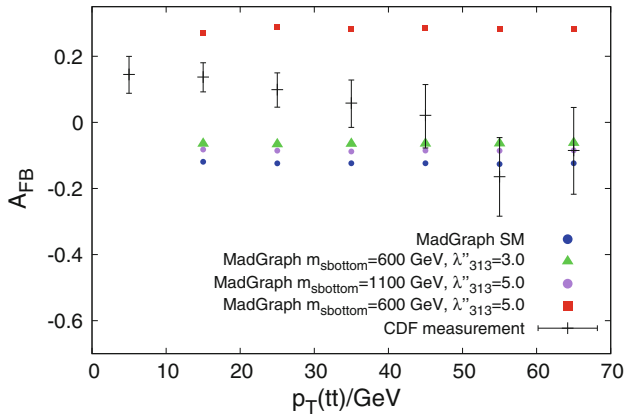

Fig. 4 Distribution of the top quark forward–backward asymmetry against the p_{T} of the $t\bar{t}$ pair at the 1.96 TeV Tevatron. The CDF result is shown [33], as well as four distributions calculated by `MadGraph5_v1_5_11`: the leading-order Standard Model $t\bar{t}j$ prediction, and predictions for $t\bar{t}j$ production via both SM and SUSY processes with a sbottom of mass 600 GeV and λ''_{313} coupling of 3.0 or 5.0, and with a sbottom of mass 1,100 GeV and λ''_{313} coupling of 5.0

$\lambda''_{313} = 5.0$. These simulations include leading-order QCD $t\bar{t}j$ production as well as tree-level processes involving the RPV sbottom. Our leading-order `MadGraph5_v1_5_11` Standard Model prediction is also shown in Fig. 4 and is compatible with the recent determination in Ref. [34], which uses an independent event generator (`HERWIG++` [39]).

Since the CDF results are unfolded, to compare to these we did not need to apply any cuts on the simulated $t\bar{t}$ plus jet system, or on any decay products of the tops. However, `MadGraph5_v1_5_11` can only simulate tree-level processes—it does not include loops—so to avoid difficulties with soft jet divergences, we imposed a lower cut of 10 GeV on the transverse momentum of the jet in our simulated events. This is why our histograms of `MadGraph5_v1_5_11` predictions in Fig. 4 do not include the first bin. At a sbottom mass of 600 GeV, the smaller coupling value shown ($\lambda''_{313} = 3.0$) falls within the region Allanach and Sridhar found which gives the correct value for the total forward–backward asymmetry, and passed other constraints that were relevant at the time. A sbottom mass of 1,100 GeV and coupling of 5.0 also falls within this region. The figure shows that the leading-order Standard Model $p_{\mathrm{T}}(t\bar{t})$ distribution is fairly flat, in apparent contradiction with the data (the χ^2-value is 60 and there are 6 degrees of freedom). All of the points in $m_{\tilde{b}_R} - \lambda''_{313}$ parameter space listed produce a flat distribution, which does not appear to be mirrored well in the data, which has the trend of decreasing $A_{FB}(t\bar{t})$ with increasing top quark pair p_{T}. The prediction of $\lambda''_{313} = 3.0$, $m_{\tilde{b}_R} = 600$ GeV has a χ^2-value of 35, and that of $\lambda''_{313} = 5.0$, $m_{\tilde{b}_R} = 1{,}100$ GeV has a χ^2-value of 42. The prediction of $\lambda''_{313} = 5.0$, $m_{\tilde{b}_R} = 600$ GeV is far above the SM prediction but has a χ^2-value of 61. For 6 degrees of freedom, each of these $m_{\tilde{b}_R} - \lambda''_{313}$ points has a p-value of less than 10^{-5}, as does our Standard Model result. We have not included theoretical errors on the `MadGraph5_v1_5_11` calculations; of course the p-values will alter somewhat if these are taken into account. Throughout this paper, we assume that the likelihood is Gaussian distributed in the observables and we use two tailed p-values to set limits.

Colour anti-triplet exchange thus has a similar status to axigluon or Z' explanations of the $A_{FB}(t\bar{t})$ measurements: $A_{FB}(t\bar{t})$ is prediction to be approximately flat in p_{T}, as is the Standard Model itself.

3 Recasting an LHC search and an LHC measurement

We now sketch the procedure whereby we calculate exclusion regions upon the relevant parameter space by recasting LHC measurements and searches in terms of the RPV light sbottom model. For each search or measurement to be reinterpreted, experimental observables for the RPV SUSY model were calculated using the matrix element event generator `MadGraph5_v1_5_11` [35] assuming a top mass of $m_t = 172.5$ GeV, the CTEQ6L1 parton distribution functions (PDFs) [40] and using the FeynRules [36] implementation of the RPV MSSM [37,38]. We define 11×11 grids in $m_{\tilde{b}_R} - \lambda''_{313}$ and $m_{\tilde{b}_R} - \lambda''_{323}$ parameter space, simulating 10,000 events at each grid point. At different grid points, the only quantities that are changed in the simulations are the mass, coupling and width of the sbottom. Predicted observables were interpolated between the grid points.

Figures 2, 3 and 6 show the BSM processes used in our simulations. (We have omitted here, but included in our simulations, diagrams which can be created from those shown by replacing all particles with their anti-particles, and vice versa). These are the diagrams for the case with a non-zero λ''_{313} coupling—for the case with a non-zero λ''_{323} coupling, every down quark in the diagrams must be instead replaced with a strange quark (and anti-down quarks with anti-strange quarks). Every process simulated involving the RPV sbottom has a $t\bar{t}$ pair in the final state. We found that the cross sections of the $t\bar{t}d$ (Fig. 3) and $t\bar{t}d\bar{d}$ processes (Fig. 6) can be sizeable enough relative to the leading-order $t\bar{t}$ diagram (Fig. 2), in certain regions of $m_{\tilde{b}_R} - \lambda''_{313}$ parameter space. They therefore need to be included in our simulations. The measurement of $t\bar{t}$ production that we use is inclusive, and so these processes contribute to it. Figure 5 shows the cross section for each set of diagrams as a function of the coupling λ''_{313} for two values of the mass of the sbottom. For the purposes of illustration, we have not included the pure QCD, nor the BSM-QCD interference contribution in Fig. 5, although we include them as appropriate later when analysing LHC data. The $t\bar{t}d$ process is seen to have a larger cross section than

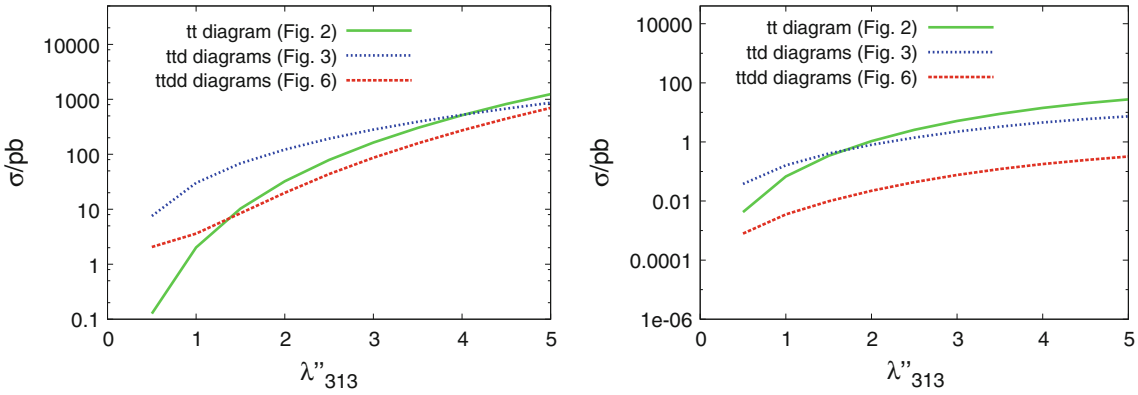

Fig. 5 Pure BSM cross sections as a function of coupling λ''_{313} for $t\bar{t}$ production events via a sbottom at the 7 TeV LHC: comparing the leading-order $t\bar{t}$ process (Fig. 2) with $t\bar{t}d$ (Fig. 3) and $t\bar{t}d\bar{d}$ (Fig. 6) processes, for two values of the sbottom mass

$t\bar{t}$ for a sbottom mass of 250 GeV and a λ''_{313} coupling less than about 4.0, and for a sbottom mass of 1,100 GeV and coupling less than about 1.5. The $t\bar{t}d$ process has a gluon replacing either a down or an anti-down quark in the initial state as compared to the $t\bar{t}$ diagram. The enhanced PDF for gluons, as opposed to anti-downs in the proton at 7–8 TeV, can outweigh the naive α_s suppression of the $t\bar{t}d$ process compared to $t\bar{t}$. (At the Tevatron, by contrast, valence anti-downs are present in the collisions, so the $t\bar{t}d$ process is a less significant correction to inclusive top pair production than at the LHC. Indeed it was not included in Allanach and Sridhar's simulations.)

As seen in Fig. 5, the $t\bar{t}d\bar{d}$ BSM process is sub-dominant to one of the other two, but it can be of the same order as the dominant process, and so we include it in our simulations. It can have two gluons in its initial state and so, similarly to the $t\bar{t}d$ process, PDF enhancements can counteract the naive suppression that is expected for higher-order diagrams.

The cross sections of processes involving the coupling λ''_{323} are always smaller than equivalent processes involving the coupling λ''_{313}, because they require strange quarks and/or anti-quarks in the initial state, as opposed to downs and/or anti-downs. Since there are no valence strange quarks in protons, but there are valence downs, the strange PDF is smaller than the down PDF for all values of x (the fraction of the proton momentum carried by the interacting parton). Consequently the excluded regions we found are smaller in the $m_{\tilde{b}_R} - \lambda''_{323}$ parameter space than in the $m_{\tilde{b}_R} - \lambda''_{313}$ parameter space.

As well as the measurements described below, we also looked at two more LHC searches. One of these was a search for contact interactions published by the CMS collaboration [41]. They displayed the inclusive jet p_{T} spectrum for jets produced in pp collisions at a centre of mass energy of 7 TeV, for jets with a p_{T} between 507 and 2,116 GeV. We tried to produce an exclusion region for the sbottom in mass–coupling parameter space using this measurement, but the cross sections for the simulated RPV SUSY events were too low (by a factor of about 15) to exclude any points within either mass–coupling parameter space grid.

We also looked at a recent search by CMS for pair production of resonances, each decaying to a top and a jet [42]. This is obviously relevant to our sbottom, which decays to a top and either a down or a strange quark. CMS looked for a bump in the invariant mass of the top and jet in events with two tops and two jets. They were searching specifically for an excited top which decays into a top and a gluon. These excited tops are very narrow, whereas our sbottom LSP is much wider, with a width given by

$$\Gamma = \frac{\lambda''^2_{3i3}(m^2_{\tilde{b}_R} - m^2_t)^2}{8\pi m^3_{\tilde{b}_R}}, \tag{4}$$

where m_t is the top quark mass. In the CMS paper, a plot is presented that gives the excluded values of the cross section of pair production of the resonance as a function of the mass of the resonance. However, this limit is based on a calculation with resonance significantly narrower than ours, and narrower resonances are easier to see against a smoothly decaying background than wider ones, so we cannot justify directly applying the limits to our model. We cannot create our own exclusion from their plot of the differential cross section as a function of the invariant mass of the top quark plus jet, because then we would need to accurately model the experimental resolution. We have, however, found one LHC measurement and one LHC search which yield strong constraints on our model. Below, we describe the measurement first.

3.1 Differential top quark transverse momentum

The first excluded regions were calculated using the differential top transverse momentum distribution in dileptonic $t\bar{t}$

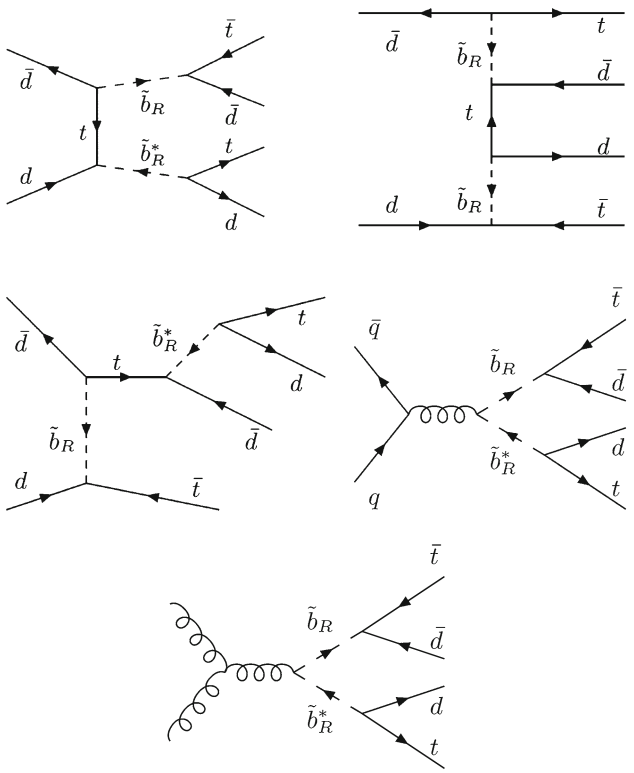

Fig. 6 Diagrams producing a $t\bar{t}$ pair as well as a down and an anti-down (order λ''^4_{313} or order $\lambda''^2_{313}\alpha_s^2$). Here, only two order $\lambda''^2_{313}\alpha_s^2$ diagrams are shown, but there are many more diagrams of the same order (all are included in simulations). Also not shown, but included in our simulations, are diagrams that can be created from these ones by replacing quarks with corresponding anti-quarks, and vice versa

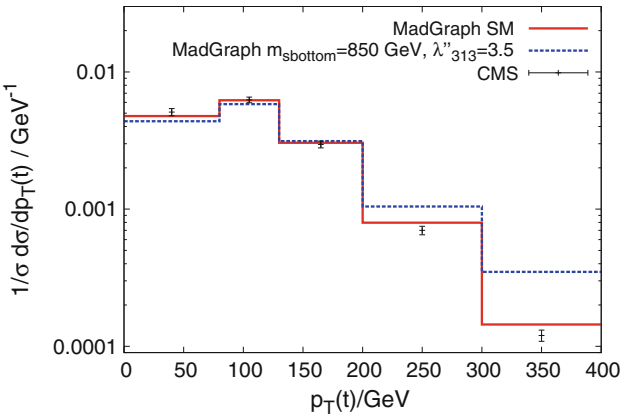

Fig. 7 Differential distribution of the p_T of the top quarks in $t\bar{t}$ 7 TeV LHC events (in which both top and anti-top decay leptonically, and the p_Ts of both are included in the distribution). The CMS measurement and its error bars are shown [43], as well as two distributions calculated by `MadGraph5_v1_5_11`. The `MadGraph5_v1_5_11` Standard Model prediction is shown as the solid histogram, and the `MadGraph5_v1_5_11` prediction for $t\bar{t}$ production via Standard Model plus sbottom induced processes as the dotted histogram, for sbottoms of mass 850 GeV and $\lambda''_{313} = 3.5$

production events as measured by the CMS collaboration at the LHC [43]. CMS measured the differential cross section of $t\bar{t}$ events as a function of the transverse momentum of the top quarks (including both top and anti-top quarks) in 5 fb^{-1} of proton–proton collisions at a centre of mass energy of 7 TeV.

The SUSY $t\bar{t}$ processes that we simulated for the λ''_{313} coupling case are shown in Figs. 2, 3 and 6. Equivalent diagrams with down quarks replaced by strange quarks were simulated for the case involving the λ''_{323} coupling. The leading-order Standard Model $t\bar{t}$ production diagram was also included.

Our simulations were performed at the parton level and we did not decay tops nor did we include parton showering. The CMS measurement is presented in their paper after having been unfolded to the full $t\bar{t}$ phase space so we are justified in comparing it directly to parton level $t\bar{t}$ simulated events without cuts.

A statistical comparison between measurement and simulation was made using the CL$_s$ test [44,45]. At each point on the parameter space grid, the differential p_T distribution of the tops was calculated and binned in the same way as in the CMS paper. The differential distribution of the top p_T is illustrated for the CMS measurement and our `MadGraph5_v1_5_11` calculations in Fig. 7. We see from the figure that the new physics contribution enhances the high $p_T(t)$ tail.

The 'background-only hypothesis' for the CL$_s$ test was taken to be the NNLO SM prediction, taken from the CMS paper. Then the SM plus sbottom prediction was taken to be the NNLO predicted histogram, minus the MadGraph SM histogram, as shown in Fig. 7, added on to the MadGraph SM plus sbottom histogram (taking into account the differing cross sections in this sum). The CL$_s$ test was used, for 4 degrees of freedom, to determine which points on the grid fell inside the 95 % confidence level exclusion regions, i.e. where the value of CL$_s$ is less than 5 % (we have normalised the area of each histogram in Fig. 7 to 1, losing one degree of freedom with respect to the number of bins).

Figure 8 shows the constraint on the $m_{\tilde{b}_R} - \lambda''_{313}$ parameter space coming from the measurement of the differential distribution of the top p_T in the dilepton channel, as labelled in the legend. The region inside the line labelled 'Allanach and Sridhar's allowed region' is taken from Ref. [30], and it is consistent with the 95 % CL regions of: the CDF and DØ data on $A_{FB}(t\bar{t})$ for low and high invariant mass bins [46], the total $t\bar{t}$ production cross section [47], the CDF differential cross section with respect to the $t\bar{t}$ invariant mass [48], and the ATLAS [49] and CMS [50] $t\bar{t}$ cross sections measured at 7 TeV. It is also consistent with early measurements of the charge asymmetry at 7 TeV by ATLAS [31] and CMS [51]. Much of the higher λ''_{313} parameter space is ruled out by the $p_T(t)$ distribution. Figure 9 shows the constraints given

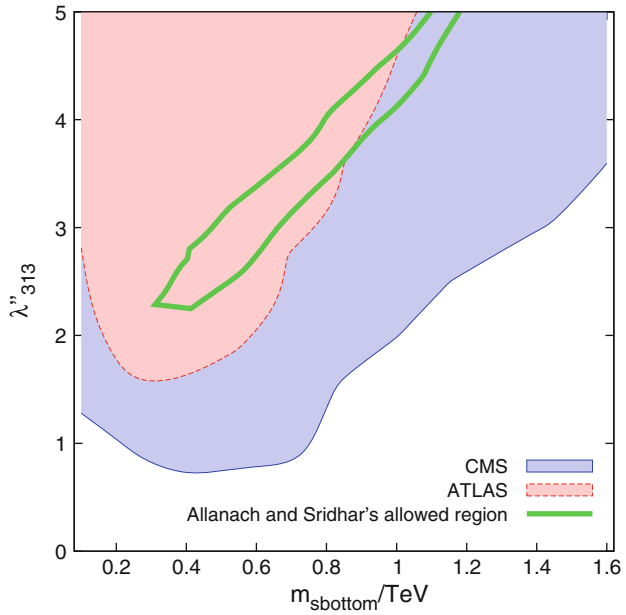

Fig. 8 $m_{\tilde{b}_R} - \lambda''_{313}$ parameter space, showing the 95 % CL exclusion regions from (**a**) the top p_T spectrum measured by CMS in 5 fb^{-1} of 7 TeV LHC collisions, marked 'CMS' [43], and (**b**) a multiple jet resonance search by ATLAS in 20.3 fb^{-1} of 8 TeV LHC collisions [52], marked 'ATLAS'

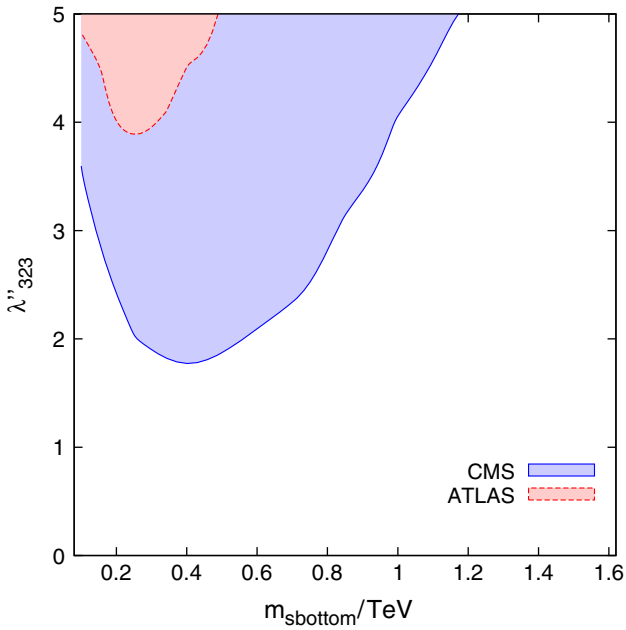

Fig. 9 $m_{\tilde{b}_R} - \lambda''_{323}$ parameter space, showing the 95 % CL exclusion regions from (**a**) the top p_T spectrum measured by CMS in 5 fb^{-1} of 7 TeV LHC collisions, marked 'CMS' [43], and (**b**) a multiple jet resonance search by ATLAS in 20.3 fb^{-1} of 8 TeV LHC collisions [52], marked 'ATLAS'

by the top p_T measurement on $m_{\tilde{b}_R} - \lambda''_{323}$ parameter space, yielding significant constraints (albeit weaker ones than on λ''_{313}).

3.2 ATLAS search for pair production of massive particles decaying into several quarks

The ATLAS collaboration recently undertook a search for the production of pairs of massive particles, each of which decays into multiple quarks, in 20.3 fb^{-1} of proton–proton collisions at $\sqrt{s} = 8$ TeV at the LHC [52]. They were looking in particular for baryon-number violating gluinos which decay to three or five quarks each. The search involved counting the number of events which contained at least seven jets all with $p_T > 80$ GeV and $|\eta| < 2.8$ (η is pseudorapidity), and with either 0, 1 or 2 b-tags (where the b-jets must have $|\eta| < 2.5$). Since our signal contains a $t\bar{t}$ pair in the final state, we used the ATLAS 2 b-tag event count to calculate an exclusion region.

Using `MadGraph5_v1_5_11`, we simulated all of the processes shown in Figs. 3 and 6 (we excluded the diagram in Fig. 2 since it cannot produce 7 partons in the final state), decaying the tops hadronically. Then for each value of the sbottom mass and coupling values investigated, the cross section was taken to be the fraction of events that passed the cuts (i.e. those which contain at least seven final-state partons each with $p_T > 80$ GeV and $|\eta| < 2.8$ of which two are b quarks with $|\eta| < 2.5$) in the simulated event samples times the production cross section, plus the background estimation given in the ATLAS paper. The number of events predicted is then this cross section multiplied by the integrated luminosity. Using the χ^2 test between the number of events found in this way and ATLAS's measured number, for each point in mass–coupling parameter space, we were able to find the regions of $m_{\tilde{b}_R} - \lambda''_{313}$ and $m_{\tilde{b}_R} - \lambda''_{323}$ parameter space that are excluded at 95 % by the ATLAS measurement. These regions are shown in Figs. 8 and 9.

4 Conclusions

We have investigated constraints on a light sbottom which couples to quarks via the R-parity violating coupling λ''_{313} or λ''_{323}. Our constraints complement recent work which focusses on baryon-number violating decays of top squarks whose mother is a gluino [7–11], which leads to the experimentally advantageous like-sign dilepton signature. Using recent LHC measurements, we have ruled out a large region in $m_{\tilde{b}_R} - \lambda''_{313}$ parameter space. This region includes the entire previously allowed parameter space region [20,30,32], which explains the anomalously high $t\bar{t}$ forward–backward asymmetry at the Tevatron [21–24]. The excluded region in $m_{\tilde{b}_R} - \lambda''_{323}$ parameter space is smaller, because processes involving the λ''_{323} coupling require strange quarks in the initial state as opposed to down quarks. The associated PDF suppression in the cross sections of processes involving the λ''_{323} coupling, relative to those involving similar values of

λ''_{313}, makes it more difficult to constrain $m_{\tilde{b}_R} - \lambda''_{323}$ parameter space.

Excluded RPV couplings are rather large (higher than about 0.7), and therefore we see that our results should be fairly robust with respect to changes to our initial simplifying assumption that the sbottom is the LSP. If the sbottom were not the LSP, the worry was that competing R-parity conserving decays would weaken our bounds. While this is in principle true, the R-parity conserving decay modes will likely be sub-dominant to the RPV decay modes for couplings higher than about 0.7, and so the effect of having a different LSP on our observables is likely to be small. For the same reason, R-parity conserving contributions to the sbottom width are likely to be small compared to Eq. 4.

Our simulations were performed at the parton level. But we can be confident that our conclusions are reliable without simulating parton showering, hadronisation and detectors, because the most constraining measurement is the CMS top p_{T} distribution, which was unfolded to the $t\bar{t}$ level.

We presented the top pair p_{T} dependence of the Tevatron forward–backward asymmetry predicted by this sbottom model (with λ''_{313} as the non-zero RPV coupling). We found it to predict a flat distribution, which does not fit CDF data well [33].

We have investigated both possibilities for a real λ''_{3j3} coupling for which the sbottom couples to a top. But there are of course other possibilities for the dominant λ''_{ij3} coupling which do not involve tops. For example the sbottom could couple to an up quark and a strange quark. In this situation, the sbottom would be more difficult to discover at the LHC, since the signal would be hiding in the extremely large jet background.

We had some trouble finding LHC searches which would be sensitive to our signal. Most of the SUSY searches are not applicable because they usually put strong lower cuts on the missing transverse momentum (MET). They also often veto leptons in the event to ensure that the MET does not come from a W boson decaying leptonically. This is because they are looking for stable LSPs which would show up as large MET, and they want to exclude events where the only MET is due to a neutrino, since such events constitute a new physics background. Since the only source of MET in our signal is neutrinos from tops decaying leptonically, a large part of our signal does not pass cuts on the R-parity conserving SUSY searches and we cannot use them to strongly constrain the model. ATLAS have recently performed a search for B-violating operators in RPV supersymmetry, but the search required kinematically accessible gluinos in the model, and their signal was same-sign dileptons, neither of which are predicted by our set up [53]. In this case, for a 100 % branching ratio of $\tilde{g} \to tbs$, the experimental limit $m_{\tilde{g}} > 900$ GeV applies [53]. The recent recasting [9] of 3.95 fb^{-1} of an 8 TeV CMS b-tags and like-sign lepton search yields $m_{\tilde{g}} > 800$ GeV [54]. Recent searches for RPV SUSY that look in particular for lepton-number violating operators [55,56] require more leptons in the final state than our signal produces, so we cannot reinterpret these to put bounds on our model. However, we expect precision top measurements to better exclude this model in the future, because processes involving these LSP sbottoms alter the differential production cross section of tops.

Acknowledgments This work has been partially supported by STFC. We thank M. Schmaltz for the initial idea. Thanks to the Cambridge Supersymmetry Working Group for helpful discussions.

References

1. B. Batell, T. Lin, L.-T. Wang, (2013). arXiv:1309.4462
2. N.-E. Bomark, S. Lola, P. Osland et al., Phys. Lett. B **677**, 62 (2009). arXiv:0811.2969
3. E. Duchovni, in *Proceedings of 32nd International Symposium on Physics in Collision (PIC 2012)*. (2013), pp. 79–92. arXiv:1305.4920
4. J.M. Butterworth, J.R. Ellis, A.R. Raklev et al., Phys. Rev. Lett. **103**, 241803 (2009). arXiv:0906.0728
5. B. Allanach, A. Barr, L. Drage et al., JHEP **0103**, 048 (2001). arXiv:hep-ph/0102173
6. C. Brust, A. Katz, S. Lawrence et al., JHEP **1203**, 103 (2012). arXiv:1110.6670
7. B. Allanach, B. Gripaios, JHEP **1205**, 062 (2012). arXiv:1202.6616
8. M. Asano, K. Rolbiecki, K. Sakurai, JHEP **1301**, 128 (2013). arXiv:1209.5778
9. J. Berger, M. Perelstein, M. Saelim et al., JHEP **1304**, 077 (2013). arXiv:1302.2146
10. Z. Han, A. Katz, M. Son et al., Phys. Rev. D **87**, 075003 (2013). arXiv:1211.4025
11. G. Durieux, C. Smith, JHEP **1310**, 068 (2013). arXiv:1307.1355
12. E. Nikolidakis, C. Smith, Phys. Rev. D **77**, 015021 (2008). arXiv:0710.3129
13. C. Csaki, B. Heidenreich, Phys. Rev. D **88**, 055023 (2013). arXiv:1302.0004
14. C. Csaki, Y. Grossman, B. Heidenreich, Phys. Rev. D **85**, 095009 (2012). arXiv:1111.1239
15. G. Krnjaic, D. Stolarski, JHEP **04**, 064 (2013). arXiv:1212.4860
16. B. Bhattacherjee, J. Evans, M. Ibe et al., Phys. Rev. D **87**, 115002 (2013). arXiv:1301.2336
17. G.F. Giudice, B. Gripaios, R. Sundrum, JHEP **1108**, 055 (2011). arXiv:1105.3161
18. P. Slavich, Nucl. Phys. B **595**, 33 (2001). arXiv:hep-ph/0008270
19. M.I. Gresham, I.-W. Kim, S. Tulin et al., Phys. Rev. D **86**, 034029 (2012). arXiv:1203.1320
20. G. Dupuis, J.M. Cline, JHEP **1301**, 058 (2013). arXiv:1206.1845
21. V. Abazov et al. (D0 Collaboration), Phys. Rev. Lett. **100**, 142002 (2008). arXiv:0712.0851
22. T. Aaltonen et al. (CDF Collaboration), Phys. Rev. Lett. **101**, 202001 (2008). arXiv:0806.2472

23. T. Aaltonen et al. (CDF Collaboration), Phys. Rev. D **83**, 112003 (2011). arXiv:1101.0034
24. V.M. Abazov et al. (D0 Collaboration), Phys. Rev. D **84**, 112005 (2011). arXiv:1107.4995
25. V. Ahrens, A. Ferroglia, M. Neubert et al., Phys. Rev. D **84**, 074004 (2011). arXiv:1106.6051
26. J.F. Kamenik, J. Shu, J. Zupan, Eur. Phys. J. C **72**, 2102 (2012). arXiv:1107.5257
27. S. Westhoff, PoS EPS-HEP **2011**, 377 (2011). arXiv:1108.3341
28. J. Aguilar-Saavedra, Nuovo Cim. **C035N3**, 167 (2012). arXiv:1202.2382
29. C. Gross, G. Marques Tavares, M. Schmaltz et al., Phys. Rev. D **87**, 014004 (2013). arXiv:1209.6375
30. B. Allanach, K. Sridhar, Phys. Rev. D **86**, 075016 (2012). arXiv:1205.5170
31. G. Aad et al. (ATLAS Collaboration), Eur. Phys. J. C **72**, 2039 (2012). arXiv:1203.4211
32. K. Hagiwara, J. Nakamura, JHEP **1302**, 100 (2013). arXiv:1205.5005
33. T. Aaltonen et al. (CDF Collaboration), Phys. Rev. D **87**, 092002 (2013). arXiv:1211.1003
34. B. Gripaios, A. Papaefstathiou, B. Webber, JHEP **1311**, 105 (2013). arXiv:1309.0810
35. J. Alwall, M. Herquet, F. Maltoni et al., JHEP **1106**, 128 (2011). arXiv:1106.0522
36. N.D. Christensen, C. Duhr, Comput. Phys. Commun. **180**, 1614 (2009). arXiv:0806.4194
37. B. Fuks, Int. J. Mod. Phys. A **27**, 1230007 (2012). arXiv:1202.4769
38. C. Duhr, B. Fuks, Comput. Phys. Commun. **182**, 2404 (2011). arXiv:1102.4191
39. M. Bahr, S. Gieseke, M. Gigg et al., Eur. Phys. J. C **58**, 639 (2008). arXiv:0803.0883
40. J. Pumplin, D. Stump, J. Huston et al., JHEP **0207**, 012 (2002). arXiv:hep-ph/0201195
41. S. Chatrchyan et al. (CMS Collaboration), Phys. Rev. D **87**, 052017 (2013). arXiv:1301.5023
42. S. Chatrchyan et al. (CMS Collaboration), CMS-PAS-B2G-12-014 (2013). arXiv:1311.5357
43. S. Chatrchyan et al. (CMS Collaboration), Eur. Phys. J. C **73**, 2339 (2013). arXiv:1211.2220
44. J. Beringer et al. (Particle Data Group), Phys. Rev. D **86**, 010001 (2012)
45. A.L. Read, J. Phys. G **28**, 2693 (2002)
46. S. Leone et al. (CDF Collaboration), Electroweak Session of Rencontres de Moriond 2012 (2012)
47. T. Aaltonen et al. (CDF and D0 Collaborations), note 9913 (2009)
48. T. Aaltonen et al. (CDF Collaboration), Phys. Rev. Lett. **102**, 222003 (2009). arXiv:0903.2850
49. G. Aad et al. (ATLAS Collaboration), ATLAS-CONF-2011-121 (2011)
50. S. Chatrchyan et al. (CMS Collaboration), CMS PAS TOP-11-003 (2011)
51. S. Chatrchyan et al. (CMS Collaboration), Phys. Lett. B **709**, 28 (2012). arXiv:1112.5100
52. G. Aad et al. (ATLAS Collaboration), ATLAS-CONF-2013-091 (2013)
53. G. Aad et al. (ATLAS Collaboration), ATLAS-CONF-2013-007, ATLAS-COM-CONF-2013-006 (2013)
54. Search for supersymmetry in events with same-sign dileptons, Technical Report CMS-PAS-SUS-12-017, CERN, Geneva (2012)
55. S. Chatrchyan et al. (CMS Collaboration), Phys. Rev. Lett. **111**, 221801 (2013). arXiv:1306.6643
56. G. Aad et al. (ATLAS Collaboration), ATLAS-CONF-2013-036 (2013)